IEEE Access
Multidisciplinary | Rapid Review | Open Access Journal

Received September 23, 2021, accepted October 3, 2021, date of publication October 6, 2021, date of current version October 18, 2021.

*Digital Object Identifier 10.1109/ACCESS.2021.3118357*

# Impact of Uneven Shading by Neighboring Buildings and Clouds on the Conventional and Hybrid Configurations of Roof-Top PV Arrays

**PRIYA RANJAN SATPATHY[1], THANIKANTI SUDHAKAR BABU[2], (Senior Member, IEEE), SATHISH KUMAR SHANMUGAM[3], LAKSHMAN NAIK POPAVATH[4], AND HASSAN HAES ALHELOU[5], (Senior Member, IEEE)**

[1]Department of Electrical Engineering, ITER, Siksha 'O' Anusandhan (Deemed to be University), Bhubaneswar 751030, India
[2]Department of Electrical and Electronics Engineering, Chaitanya Bharati Institute of Technology, Hyderabad 500075, India
[3]Department of Electrical and Electronics Engineering, M. Kumarasamy College of Engineering, Karur 639113, India
[4]Department of Electrical and Electronics Engineering, Vasireddy Venkatadri Institute of Technology, Nambur 522509, India
[5]Department of Electrical Power Engineering, Faculty of Mechanical and Electrical Engineering, Tishreen University, Lattakia 2230, Syria

Corresponding authors: Hassan Haes Alhelou (alhelou@ieee.org) and Thanikanti Sudhakar Babu (sudhakarbabu66@gmail.com)

The work of Priya Ranjan Satpathy was supported by the Council of Scientific and Industrial Research (CSIR), Government of India, during the Senior Research Fellow tenure under Grant 09/0969(11258)/2021-EMR-I.

**ABSTRACT** Partial shading is the commonly encountered scenario of building roof-top based PV arrays that mainly occur due to the shadow of the neighbouring buildings and clouds resulting in unexpected losses and deteriorated system performance. The arrays are connected in various configurations to enhance the system performance during shading. In this paper, various conventional and hybrid interconnection configurations based on series-parallel (SP), bridge-linked (BL), and total cross tied (TCT) topologies of the roof-top PV arrays are examined under various partial shading scenarios caused by the neighbouring building and clouds. The investigation is done for a 9 × 9 roof-top array in MATLAB/Simulink environment considering various comparison parameters. It has been found that during 1.23%, 7.40%, 11.11%, 17.75%, 18.51%%, 22.22%, and 24.69% of total array shading, SP generated the maximum power whereas, during 30.86%, 61.72% shading, TCT has the generated only a slightly higher power as compared to SP. Hence, the study concludes that the configurations have a puny effect on the power generation of the arrays during uneven shading patterns caused by buildings and clouds.

**INDEX TERMS** Array configurations, mismatch loss, partial shading, photovoltaic, power generation, and roof-top PV system.

## LIST OF ABBREVIATIONS

| | |
|---|---|
| **PV** | Photovoltaic. |
| **SP** | Series-Parallel. |
| **BL** | Bridge-Linked. |
| **TCT** | Total Cross Tied. |
| **SP-SP** | Series Parallel-Series Parallel. |
| **SP-BL** | Series Parallel-Bridge Linked. |
| **SP-TCT** | Series Parallel-Total Cross Tied. |
| **BL-SP** | Bridge Linked-Series Parallel. |
| **BL-BL** | Bridge Linked- Bridge Linked. |
| **BL-TCT** | Bridge Linked-Total Cross Tied. |
| **TCT-SP** | Total Cross Tied-Series Parallel. |
| **TCT-BL** | Total Cross Tied-Bridge Linked. |
| **TCT-TCT** | Total Cross Tied-Total Cross Tied. |
| **P∼V** | Power∼Voltage. |
| **STC** | Standard Testing Condition. |
| **G** | Solar Irradiance. |
| $\mathbf{G_{STC}}$ | Solar Irradiance at STC. |
| **D** | Diode. |
| $\mathbf{I_{Ph}}$ | Photo-generated Current. |
| $\mathbf{I_O}$ | Diode Current. |
| **k** | Boltzmann Constant. |
| **T** | Module Temperature. |
| **q** | Electron charge. |
| $\mathbf{K_I}$ | Short-circuit current temperature co-efficient. |
| **MPP** | Maximum Power Point. |
| **MPPT** | Maximum Power Point Tracking. |
| $\mathbf{P_M}$ | Power at MPP. |

The associate editor coordinating the review of this manuscript and approving it for publication was Lin Zhang.

| | |
|---|---|
| $\mathbf{V_M}$ | Voltage at MPP. |
| $\mathbf{I_M}$ | Current at MPP. |
| $\mathbf{V_{OC}}$ | Open-Circuit Voltage. |
| $\mathbf{I_{SC}}$ | Short-Circuit Current. |
| **ML** | Mismatch Loss. |
| $\mathbf{P_{Unshaded}}$ | Power at unshaded scenario. |
| $\mathbf{P_{Shaded}}$ | Power at shaded scenario. |
| $\mathbf{P_T}$ | Theoretical Power. |
| $\mathbf{MPP_{First}}$ | Maximum Power Point at first peak. |
| $\mathbf{MPP_{Actual}}$ | Actual Maximum Power Point. |
| **PL** | Power Loss. |
| **TL** | Tracking Loss. |
| $\eta_o$ | Operational Efficiency. |
| $\eta_c$ | Conversion Efficiency. |
| **A** | Area of Module. |
| **W** | Watt. |
| **kW** | Kilowatt. |
| **V** | Voltage. |
| **A** | Ampere. |
| $\mathbf{I_{PV}}$ | Output Current of Module. |
| $\mathbf{I_{PV\_STC}}$ | Output Current of Module at STC. |
| $\mathbf{V_{PV}}$ | Output Voltage of Module. |
| $\mathbf{R_S}$ | Series Resistance. |
| $\mathbf{R_{Sh}}$ | Shunt Resistance. |
| $\mathbf{V_t}$ | Thermal Voltage. |
| **n** | Diode factor. |

## I. INTRODUCTION

The demand for solar photovoltaic (PV) generation is continuously rising at a faster pace due to higher source availability, low maintenance and higher reliability. However, the higher setup cost and larger land requirement of the PV system has inspired the consumers to opt for a roof-top based system to reduce extra land cost and higher initial cost [1]. However, the PV array constituents of modules installed at the building roof-top encounter a critical scenario of partial shading that is mainly caused by the neighbouring buildings and cloud passage [2]. These scenarios can reduce the overall performance of the array by either generating very low power output or creating a hotspot among the shaded modules whose long-term existence leads to physical damage to the PV module [3]. Generally, for hotspot reduction in modules, bypass diodes are implemented in parallel with the modules that allow the current generated by unshaded modules to flow through it preventing hotspots [4]. However, in most of the shading cases, the bypass diodes distort the characteristics curves of the array by forming multiple peaks having lower power peak at the first position and hence, mislead the maximum power point tracker algorithms towards false tracking [4]. Various MPPT algorithms for effective tracking of true maximum power point (MPP) are proposed in the literature and tested under various shading scenarios [5]. Some of these algorithms follow techniques such as fusion fly [6], Harish hawk optimization [7], grasshopper optimization [8], salp-swarm optimization [9], dynamic particle method [10], hybrid evolutionary methods [11], improved grey wolf optimization [12], bat algorithm [13], chaotic flower pollination [14], marine predators algorithm [15] etc. But, the adoption of these algorithms in the PV system can add to system cost and complexity due to the requirement of large numbers of switches, sensors, powerful micro-controllers and complex algorithms. Also, the algorithms encounter reliability issues under fluctuating or complex shading cases by sometimes tracking the false MPP.

Hence, to mitigate the partial shading issues, module interconnection configuration and reconfiguration among the modules is in the current trend [16]. Generally, modules in a PV array are either connected in series or series-parallel configurations based on the requirement among which series-parallel (SP) has gained wide acceptance for the roof-top system due to the low loss factors [17]. Besides these, bridge-linked (BL) and total cross tied (TCT) are conventionally widely accepted for effective shading mitigation in PV arrays that require extra wires and knots connected across the modules to disperse the current throughout the array [18]. Various studies have been performed in the literature to study the effectiveness of these configurations under partial shading and found that the TCT configuration excelled in the performance during all shading scenarios by reducing the losses caused by shading [19]–[21]. However, the study shows that the configurations have a minimal effect on the mismatch losses caused by the moving clouds [22]. Recently, reconfiguration techniques are playing a major role in combatting the effect of partial shading that adopt the principle of either changing the electrical connection or placement of PV modules to disperse the effect of shading in the entire array [23]. Some of these techniques include: shade dispersion scheme [24], magic square [25], SDP [26], SD-PAR [27], optimal Sudoku [28], fixed electrical reconfiguration [29], Lo Shu technique [30], etc. However, these techniques directly or indirectly adopt the existing TCT configuration and create wiring complexities and difficulties in fault diagnosis. Hence, these techniques remain inapplicable for most of the system installations. Various configurations based on hybridization of SP, BL, HC and TCT have been proposed and tested under shading scenarios [31]. The hybrid topologies i.e. bridge-linked honey-comb (BLHC), bridge-linked total-cross-tied (BLTCT) and series-parallel total-cross-tied (SPTCT) are studied under shading and found that BLHC has a similar performance to that of TCT with less wiring complexities [32]. All the above interconnection topologies are generally studied under various even types of partial shading patterns such as row or column shadings. However, in the real-time environment, the considered patterns are quite unrealistic as the arrays encounter uneven shading patterns caused by the buildings or clouds especially in case of roof-top systems. Also, the arrays operate under different temperatures of the shaded and unshaded modules which are not considered in the above studies.

Hence, in this paper, the above research gap has been addressed for conventional and hybrid array configurations

by considering various realistic uneven shading scenarios caused by the shadow of buildings and clouds in roof-top systems. Also, the temperature differences between the shaded and unshaded modules during partial shading is considered for approximate estimation of power generation. The conventional configurations include series-parallel (SP), bridge-linked (BL) and total-cross tied (TCT) whereas SP-SP, SP-BL, SP-TCT, BL-SP, BL-BL, BL-TCT, TCT-SP, TCT-BL and TCT-TCT are hybrid configurations. The entire study is done in the MATLAB/Simulink environment for a 9 × 9 PV array having sub-arrays of size 3 × 3 (for hybrid configurations) with a total system size of 26.3kW installed at the roof-top of a residential building. The performance of the configurations has been studied in terms of power-voltage (P∼V) characteristics curves, power generation, mismatch losses, power losses, tracking losses, number of peaks in the P∼V curves, operational efficiency, conversion efficiency, extra wires and knots requirement.

## II. SYSTEM DESCRIPTION

### A. MODELING OF PV MODULE

A PV module mainly comprises of a number of cells that are semiconductors to generate electricity from solar irradiance (G) by mean of the photoelectric effect represented by a current source with a parallel diode (D) and some resistances. The equivalent electrical circuit of the module is depicted in FIGURE 1 where $I_{Ph}$ is the photogenerated current, $I_{PV}$ is the output current, $V_{PV}$ is the output voltage, $R_S$ is the series resistance and $R_{Sh}$ is the shunt resistance of the module.

$$I_{PV} = I_{Ph} - I_o\left[\exp\left(V_{PV} + R_s I_{pv}/V_t\right) - 1\right] - \left[\left(V_{pv} + I_{pv}R_s\right)/R_{Sh}\right] \quad (1)$$

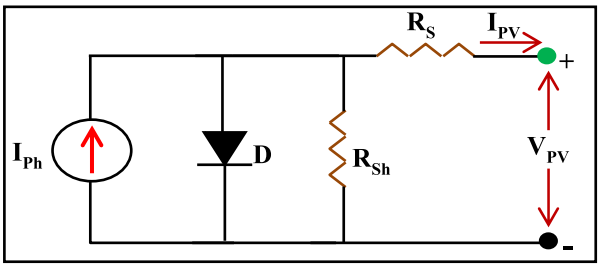


**FIGURE 1.** Equivalent circuit of a PV module.

The mathematical expression to model the PV cells has been given in equation (1) where $I_O$ symbolizes diode current, $I_{ph} = G/G_{STC} * \left(I_{PV\_STC} + K_I \Delta T\right)$ indicate photonic current, $V_t = nkT/q$ represents the thermal voltage, n, k, T, q, $K_I$, G and $G_{STC}$ symbolizes diode factors, Boltzmann's constant, module temperature, electron charge, short-circuit current temperature coefficient, irradiance received by the module, and irradiance at the standard testing condition (STC) respectively.

The specification of the module used in the study at standard testing condition (STC) i.e. 1000W/m$^2$ and 25°C has been represented in TABLE 1. In this study, eighty-one modules are connected in different configurations to form the PV arrays.

**TABLE 1.** Specification of the module at STC (1000W/m$^2$ and 25°C).

| Parameters | Rating at STC |
|---|---|
| Power at MPP ($P_M$) | 325 W |
| Voltage at MPP ($V_M$) | 37.80 V |
| Current at MPP ($I_M$) | 8.60 A |
| Open-Circuit Voltage ($V_{OC}$) | 46.40 V |
| Short-Circuit Current ($I_{SC}$) | 9.20 A |
| No. of Series Connected Cells | 72 |

### B. CONVENTIONAL 9 × 9 ARRAY INTERCONNECTION CONFIGURATIONS

Basically, modules are electrically connected in various configurations to achieve the desired voltage and current output. Series-parallel (SP) is the most common and widely accepted interconnection configuration where several modules are connected in the series to increase the system voltage output forming string and similar strings are connected in parallel for higher current output resulting in higher power output. The bridge-linked (BL) configuration is formed by connecting the wire ties across the series-parallel connected modules in a bridging manner. Total cross tied (TCT) configuration can be obtained by connecting wire ties across each junction (or positive and negative connection knot) of the PV modules that provide an extra path for the higher current generated by the unshaded modules to flow through. The schematic diagrams of 9 × 9 PV arrays with SP, BL and TCT configurations have been shown in FIGURE 2 (a), (b), and (c) respectively. The arrays generated a maximum power of 26.325kW with 340.2V, 77.40A, 417.60V and 86.4A as maximum voltage ($V_M$), maximum current ($I_M$), open-circuit voltage ($V_{OC}$), and short-current ($I_{SC}$) respectively at STC.

### C. HYBRID 9 × 9 ARRAY INTERCONNECTION CONFIGURATIONS

In this study, various hybrid PV array configurations based on the conventional configurations i.e. SP, BL, and TCT have been tested under the various neighbouring building and cloud-based shading scenarios. The hybrid configurations are formed by dividing the 9 × 9 PV array into 9 different blocks (called sub-arrays) having 9 modules in each (3 × 3 array) as shown in FIGURE 3. The interconnection configurations are applied to the sub-arrays and then sub-array blocks are connected in different architectures forming the hybrid interconnection configurations.

The hybrid configurations considered in the study mainly include SP-SP, SP-BL, SP-TCT, BL-SP, BL-BL, BL-TCT, TCT-SP, TCT-BL, and TCT-TCT as shown in FIGURE 4. In SP-SP, SP-BL and SP-TCT, the modules of the sub-arrays are connected in a common configuration i.e. SP whereas the sub-arrays are connected in different configurations such as SP, BL and TCT. Similarly, in the case of BL-SP, BL-BL

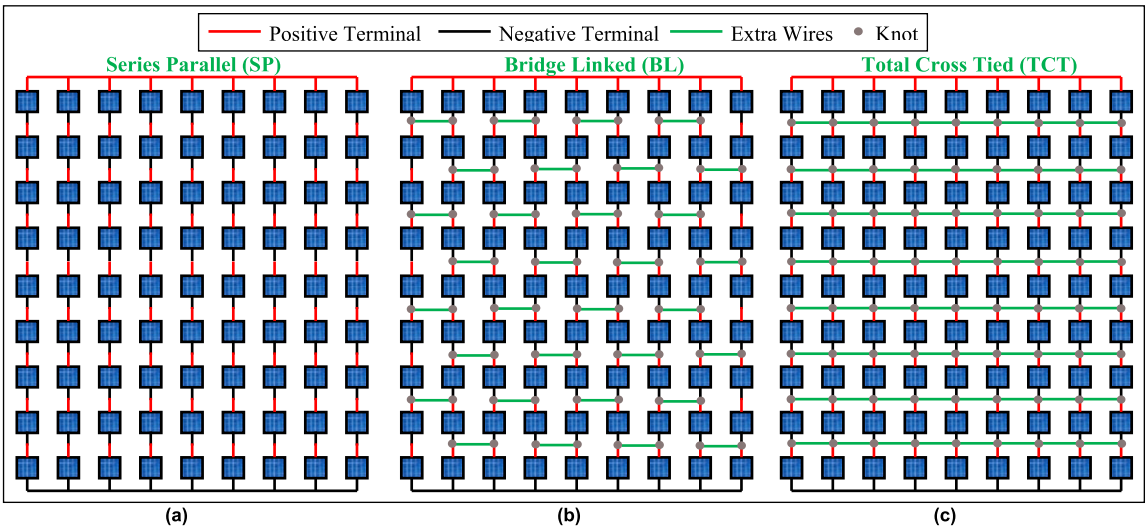


**FIGURE 2.** Schematic representation of a 9 × 9 PV array with different conventional module interconnection configurations. (a) Series-parallel (SP), (b) Bridge-linked (BL), and (c) Total cross tied (TCT).

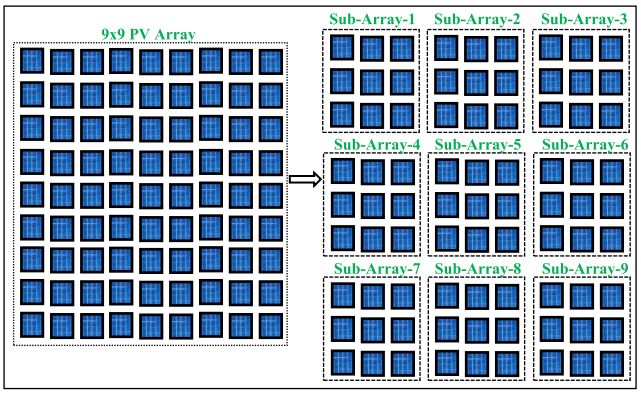


**FIGURE 3.** Evolution of 3 × 3 sub-arrays from 9 × 9 PV array.

and BL-TCT, modules of the sub-arrays are connected in BL with sub-arrays connected in SP, BL and TCT whereas in the case of TCT-SP, TCT-BL and TCT-TCT, TCT is the common configuration for the modules of the sub-arrays and the sub-arrays are connected in SP, BL and TCT configurations.

### D. PERFORMANCE COMPARISON PARAMETERS

The performance of various PV modules interconnection configurations under partial shading is compared using various parameters such as power generation, mismatch loss, power loss, tracking loss, number of peaks in P∼V curves, operational efficiency, power conversion efficiency, extra wires and knots requirement [33].

The P∼V characteristics curve of a configuration can be extracted by using a variable resistor in the simulation whereas the number of peaks and location of actual MPP depends upon the nature and pattern of shading. The power ($P_M$) generation of PV array during particular shading is the product of maximum voltage ($V_M$) and current ($I_M$) given as

$$P_M = V_M \times I_M \tag{2}$$

The mismatch loss (ML) is the difference between the maximum power generated by the PV array under unshaded scenario ($P_{Unshaded}$) and shaded ($P_{Shaded}$) scenario given as

$$ML = P_{Unshaded} - P_{Shaded} \tag{3}$$

The power loss (PL) is calculated as the difference between the theoretical power ($P_T$) and actual power generated by the array under the shaded scenario ($P_{Shaded}$) represented in equation (4). The theoretical power of the array is the sum of power generated by individual modules during shading scenarios.

$$PL = P_T - P_{Shaded} \tag{4}$$

The tracking loss (TL) is the power loss encountered by the maximum power point tracking (MPPT) algorithms due to false tracking of local MPP (if lies in the first position) instead of actual MPP of the array and can be determined as

$$TL = MPP_{First} - MPP_{Actual} \tag{5}$$

The operational efficiency ($\eta_o$) of the PV array can be calculated as the percentile of the ratio between output power during shading to the input i.e. product of receiving irradiance (G) and area of the modules (A) given as

$$\eta o = \frac{P_{Shaded}}{G \times A} \times 100 \tag{6}$$

The power conversion efficiency ($\eta_c$) is the percentile of the ratio between the actual maximum power generated by the array during the unshaded scenario to the theoretical power i.e.

$$\eta_c = \frac{P_{Shaded}}{P_T} \times 100 \tag{7}$$

The wires required to form the BL and TCT configurations from the SP configuration are mainly termed as the extra

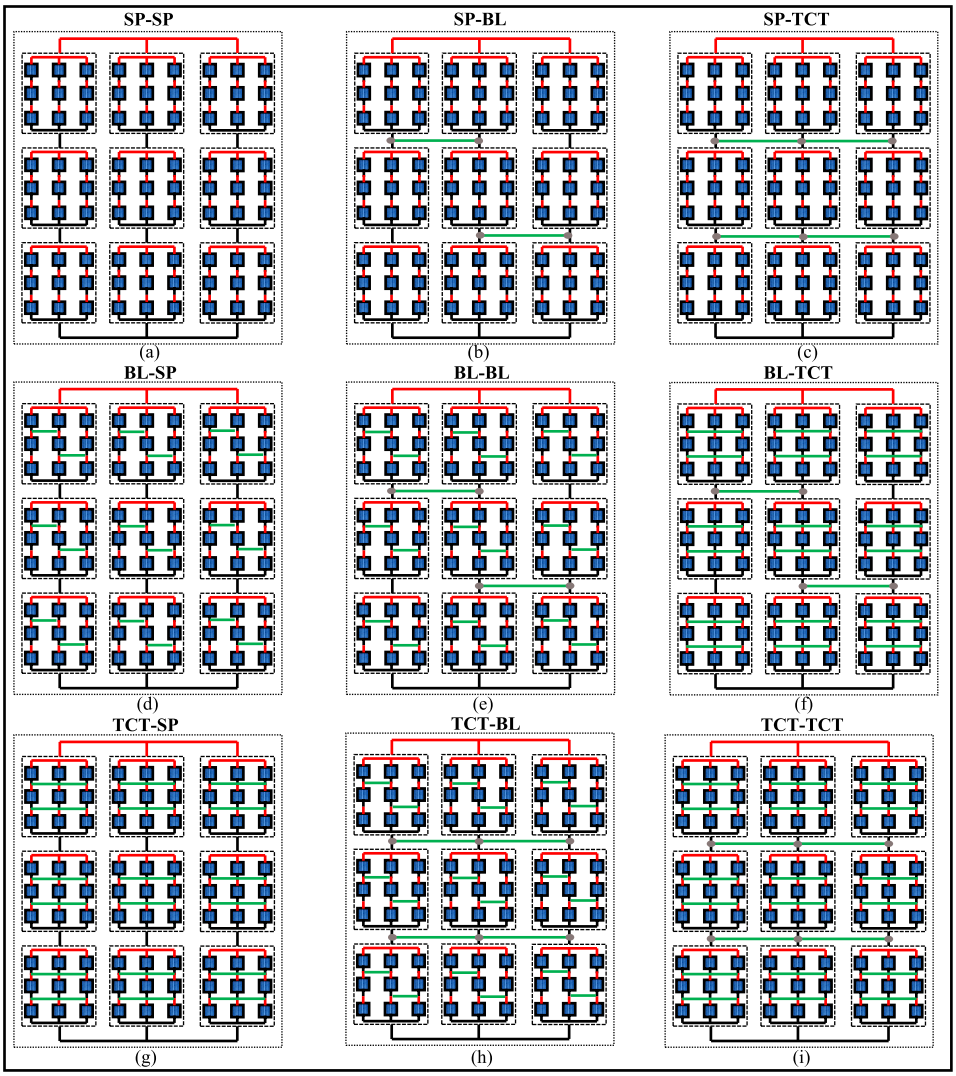


**FIGURE 4.** Various hybrid module interconnection configurations for 9 × 9 PV arrays.

wires connected to junctions using knots as represented in FIGURE 5. This parameter is mainly used to compare the redundancy level and wiring losses of the configurations. The higher the wires and knots count, the higher will be the wiring losses and redundancy level in the system.

## III. PERFORMANCE EVALUATION UNDER BUILDING SHADOW SCENARIO

The conventional module interconnection configurations i.e. SP, BL, and TCT are studied under various real-time based shading scenarios that are mainly caused by the nearby buildings. The shading scenario has been categorized into four cases where the shadow formed by the nearby building changes concerning the time of the day and position of the sun covering a total area of 1.96% to 61.72% of the 9 × 9 PV array. The 9 × 9 PV arrays have generated a maximum power of 22.88kW during shadow-free or unshaded conditions i.e. 800W/m$^2$ irradiance and 45°C module operating temperature. The irradiance and operating temperature of the modules operating under shading scenario have been considered as 200W/m$^2$ and 35°C respectively.

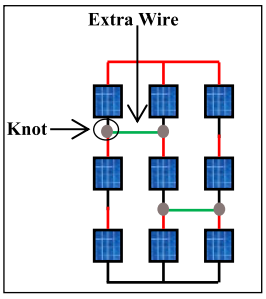


**FIGURE 5.** Schematic diagram of a 3 × 3 sub-array representing extra wires and knots required in PV array configurations.

The building shading case A has been shown in FIGURE 6 (a) where the shadow of the neighbouring building covered one module i.e.1.23% of the array. The P∼V characteristics of the array with SP, BL and TCT configurations

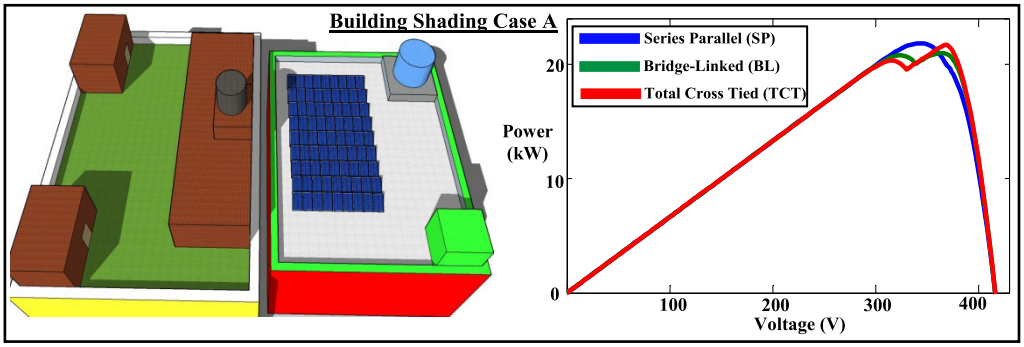


**FIGURE 6.** Neighbouring building shading case A for roof-top based 9 × 9 PV array configurations. (a) Shading scenario (drawn using SketchUp tool) and, (b) P∼V characteristics curves.

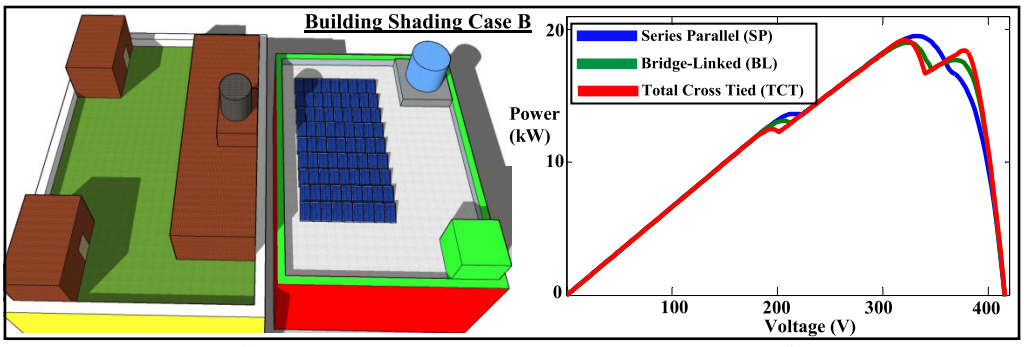


**FIGURE 7.** Neighbouring building shading case B for roof-top based 9 × 9 PV array configurations. (a) Shading scenario (drawn using SketchUp tool) and, (b) P∼V characteristics curves.

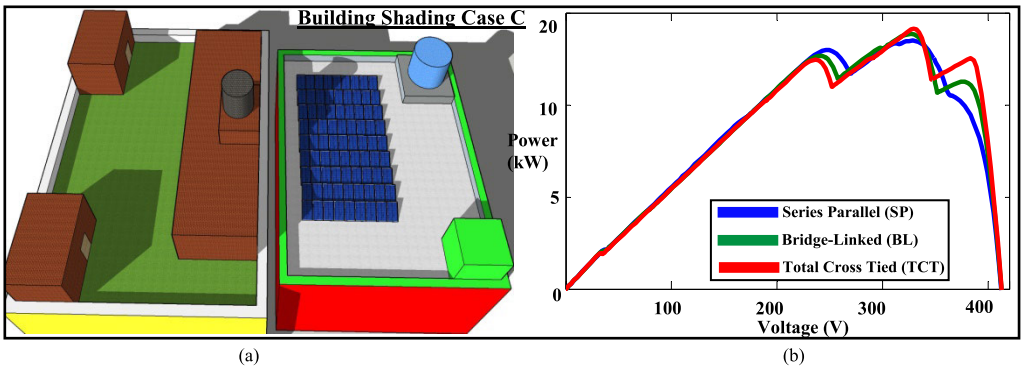


**FIGURE 8.** Neighbouring building shading case C for roof-top based 9 × 9 PV array configurations. (a) Shading scenario (drawn using SketchUp tool) and, (b) P∼V characteristics curves.

has been depicted in FIGURE 6 (b) where the SP array exhibited a convex characteristics curve and the other two i.e. BL and TCT have non-convex curves with two peaks. The theoretical power generation of the array during shading case A has been calculated as 22.46kW. The power output of SP is higher i.e. 21.84kW as compared to TCT (21.68kW) and BL (20.97kW). The mismatch losses of the SP, BL and TCT configurations are found as 1.04kW, 1.91kW and 1.20kW whereas the power losses have been calculated as 0.62kW, 1.49kW and 0.78kW respectively. The SP has the highest operation and power conversion efficiencies of 19.87% and 97.23% as compared to the BL (19.08% and 93.36%) and TCT (19.72% and 96.52%) respectively. The SP encountered zero MPPT tracking loss due to the presence of a single peak in the P∼V curve however, the tracking losses of BL and TCT have been found as 0.19kW and 1.38kW due to the presence of multiple peaks with true MPP at the second position of the characteristics curves. Hence, during this particular kind

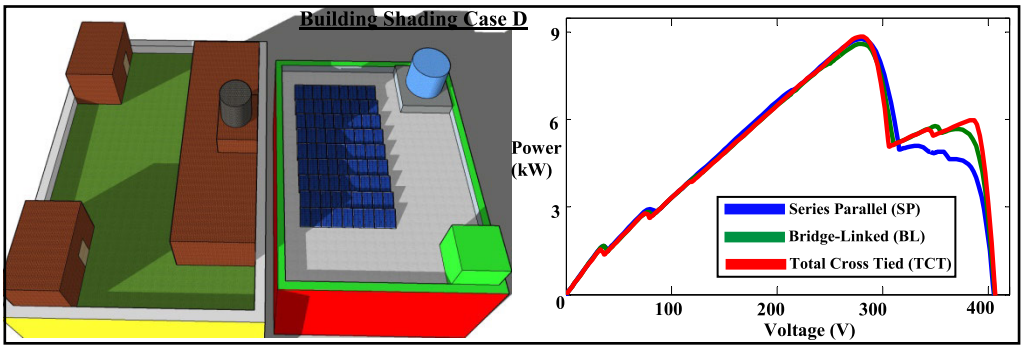


**FIGURE 9.** Neighbouring building shading case D for roof-top based 9 × 9 PV array configurations. (a) Shading scenario (drawn using SketchUp tool) and, (b) P∼V characteristics curves.

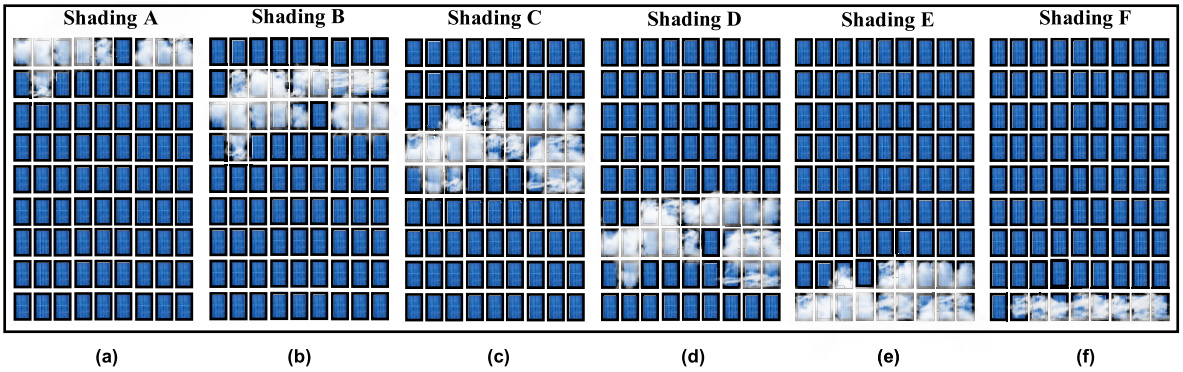


**FIGURE 10.** Cloud shadow scenarios considered for 9 × 9 PV array configurations. (a) Shading case A (11.11%), (b) Shading case B (30.86%), (c) Shading case C (24.69%), (d) Shading case D (22.22%), (e) Shading case E (18.51%), and (f) Shading case F (11.11%).

**TABLE 2.** Performance summarization of different conventional PV array configurations during building shadow cases.

| *Building Shading Case A* | | | | | | | | |
|---|---|---|---|---|---|---|---|---|
| **Configuration** | **$P_T$ (kW)** | **$P_M$ (kW)** | **ML (kW)** | **PL (kW)** | **TL (kW)** | **$\eta_o$ (%)** | **$\eta_c$ (%)** | **No. of Peaks** |
| **SP** | 22.46 | 21.84 | 1.04 | 0.62 | 0 | 19.87 | 97.23 | 1 |
| **BL** | | 20.97 | 1.91 | 1.49 | 0.19 | 19.08 | 93.36 | 2 |
| **TCT** | | 21.68 | 1.20 | 0.78 | 1.38 | 19.72 | 96.52 | 2 |
| *Building Shading Case B* | | | | | | | | |
| **Configuration** | **$P_T$ (kW)** | **$P_M$ (kW)** | **ML (kW)** | **PL (kW)** | **TL (kW)** | **$\eta_o$ (%)** | **$\eta_c$ (%)** | **No. of Peaks** |
| **SP** | 21.38 | 19.51 | 3.37 | 1.87 | 5.85 | 17.75 | 91.25 | 3 |
| **BL** | | 19.02 | 3.86 | 2.36 | 5.90 | 17.30 | 88.96 | 3 |
| **TCT** | | 19.20 | 3.68 | 2.18 | 6.70 | 17.47 | 89.80 | 3 |
| *Building Shading Case C* | | | | | | | | |
| **Configuration** | **$P_T$ (kW)** | **$P_M$ (kW)** | **ML (kW)** | **PL (kW)** | **TL (kW)** | **$\eta_o$ (%)** | **$\eta_c$ (%)** | **No. of Peaks** |
| **SP** | 20.71 | 13.49 | 9.39 | 7.22 | 0.52 | 12.27 | 65.13 | 4 |
| **BL** | | 13.84 | 9.04 | 6.87 | 1.16 | 12.59 | 66.82 | 4 |
| **TCT** | | 14.14 | 8.74 | 6.57 | 12.22 | 12.86 | 68.27 | 4 |
| *Building Shading Case D* | | | | | | | | |
| **Configuration** | **$P_T$ (kW)** | **$P_M$ (kW)** | **ML (kW)** | **PL (kW)** | **TL (kW)** | **$\eta_o$ (%)** | **$\eta_c$ (%)** | **No. of Peaks** |
| **SP** | 12.57 | 8.76 | 14.12 | 3.81 | 7.1 | 7.97 | 69.68 | 7 |
| **BL** | | 8.60 | 14.28 | 3.97 | 6.94 | 7.82 | 68.41 | 5 |
| **TCT** | | 8.86 | 14.02 | 3.71 | 7.31 | 8.06 | 70.48 | 5 |

of shading case, the SP configuration has shown excellence over BL and TCT.

The building shading case B has been represented in FIGURE 7 (a) where 7.40% of the array encountered shadow due to the shadow of the nearby building. The total theoretical power generation of the array during this shadow condition has been calculated as 21.38kW. The P∼V characteristics curves of the SP, BL and TCT array configurations have been depicted in FIGURE 7 (b) where SP (19.51kW) has generated a significantly higher power than that of

**TABLE 3.** Performance summarization of different hybrid PV array configurations during building shadow cases.

| *Building Shading Case A* | | | | | | | | |
|---|---|---|---|---|---|---|---|---|
| **Configuration** | **$P_T$ (kW)** | **$P_M$ (kW)** | **ML (kW)** | **PL (kW)** | **TL (kW)** | **$\eta_o$ (%)** | **$\eta_c$ (%)** | **No. of Peaks** |
| **SP-SP** | 22.46 | 21.28 | 1.60 | 1.18 | 0 | 19.36 | 94.76 | 2 |
| **SP-BL** | | 21.10 | 1.78 | 1.36 | 0.25 | 19.19 | 93.94 | 2 |
| **SP-TCT** | | 21.27 | 1.61 | 1.19 | 0.53 | 19.35 | 94.70 | 2 |
| **BL-SP** | | 21.10 | 1.78 | 1.36 | 0 | 19.19 | 93.94 | 2 |
| **BL-BL** | | 21.14 | 1.74 | 1.32 | 0.49 | 19.23 | 94.12 | 2 |
| **BL-TCT** | | 21.20 | 1.68 | 1.26 | 0.65 | 19.29 | 94.39 | 2 |
| **TCT-SP** | | 21.05 | 1.83 | 1.41 | 0 | 19.15 | 93.72 | 2 |
| **TCT-BL** | | 21.14 | 1.74 | 1.32 | 0.53 | 19.23 | 94.12 | 2 |
| **TCT-TCT** | | 21.30 | 1.58 | 1.16 | 0.80 | 19.38 | 94.83 | 2 |
| *Building Shading Case B* | | | | | | | | |
| **Configuration** | **$P_T$ (kW)** | **$P_M$ (kW)** | **ML (kW)** | **PL (kW)** | **TL (kW)** | **$\eta_o$ (%)** | **$\eta_c$ (%)** | **No. of Peaks** |
| **SP-SP** | 21.38 | 19.76 | 3.12 | 1.62 | 6.50 | 17.97 | 92.42 | 3 |
| **SP-BL** | | 19.09 | 3.79 | 2.29 | 5.83 | 17.37 | 89.28 | 3 |
| **SP-TCT** | | 19.16 | 3.72 | 2.22 | 6.20 | 17.43 | 89.61 | 3 |
| **BL-SP** | | 19.94 | 2.94 | 1.44 | 6.88 | 18.14 | 93.26 | 3 |
| **BL-BL** | | 19.10 | 3.78 | 2.28 | 6.04 | 17.37 | 89.33 | 3 |
| **BL-TCT** | | 19.19 | 3.69 | 2.19 | 6.43 | 17.46 | 89.75 | 3 |
| **TCT-SP** | | 20.00 | 2.88 | 1.38 | 6.98 | 18.19 | 93.54 | 3 |
| **TCT-BL** | | 19.10 | 3.78 | 2.28 | 6.09 | 17.37 | 89.33 | 3 |
| **TCT-TCT** | | 19.20 | 6.68 | 2.18 | 6.49 | 17.47 | 89.80 | 3 |
| *Building Shading Case C* | | | | | | | | |
| **Configuration** | **$P_T$ (kW)** | **$P_M$ (kW)** | **ML (kW)** | **PL (kW)** | **TL (kW)** | **$\eta_o$ (%)** | **$\eta_c$ (%)** | **No. of Peaks** |
| **SP-SP** | 20.71 | 14.60 | 8.28 | 6.11 | 2.05 | 13.28 | 70.49 | 3 |
| **SP-BL** | | 14.59 | 8.29 | 6.12 | 2.15 | 13.27 | 70.44 | 3 |
| **SP-TCT** | | 14.46 | 8.42 | 6.25 | 2.15 | 13.15 | 69.82 | 3 |
| **BL-SP** | | 14.45 | 8.43 | 6.26 | 1.85 | 13.14 | 69.77 | 3 |
| **BL-BL** | | 14.44 | 8.44 | 6.27 | 1.96 | 13.13 | 69.72 | 3 |
| **BL-TCT** | | 14.32 | 8.56 | 6.39 | 1.96 | 13.02 | 69.14 | 3 |
| **TCT-SP** | | 14.50 | 8.38 | 6.21 | 1.88 | 13.19 | 70.01 | 3 |
| **TCT-BL** | | 14.49 | 8.39 | 6.22 | 2.06 | 13.18 | 69.96 | 3 |
| **TCT-TCT** | | 14.37 | 8.51 | 6.34 | 1.99 | 13.07 | 69.38 | 3 |
| *Building Shading Case D* | | | | | | | | |
| **Configuration** | **$P_T$ (kW)** | **$P_M$ (kW)** | **ML (kW)** | **PL (kW)** | **TL (kW)** | **$\eta_o$ (%)** | **$\eta_c$ (%)** | **No. of Peaks** |
| **SP-SP** | 12.57 | 8.76 | 14.12 | 3.81 | 5.86 | 7.97 | 69.68 | 5 |
| **SP-BL** | | 8.80 | 14.08 | 3.77 | 5.23 | 8.00 | 70.00 | 5 |
| **SP-TCT** | | 8.56 | 14.32 | 4.01 | 5.65 | 7.78 | 68.09 | 5 |
| **BL-SP** | | 8.76 | 14.12 | 3.81 | 5.86 | 7.97 | 69.68 | 5 |
| **BL-BL** | | 8.80 | 14.08 | 3.77 | 5.23 | 8.00 | 70.00 | 5 |
| **BL-TCT** | | 8.58 | 14.30 | 3.99 | 5.63 | 7.80 | 68.25 | 5 |
| **TCT-SP** | | 8.76 | 14.12 | 3.81 | 5.86 | 7.97 | 69.68 | 5 |
| **TCT-BL** | | 8.80 | 14.08 | 3.77 | 5.23 | 8.00 | 70.00 | 5 |
| **TCT-TCT** | | 8.59 | 14.29 | 3.98 | 5.62 | 7.81 | 68.33 | 5 |

TCT (19.20kW) and BL (19.02kW). Also, the SP has the lowest mismatch and power losses of 3.37kW and 1.87kW respectively as compared to the TCT (3.68kW and 2.18kW) and BL (3.86kW and 2.36kW). The tracking losses of SP, BL and TCT have been found as 5.85kW, 5.90kW and 6.70kW respectively as all the configurations exhibited non-convex curves with three peaks having local MPP at the first position. The SP configuration has the highest operation and conversion efficiencies i.e. 17.75% and 91.25% respectively than BL (17.30% and 88.96%) and TCT (17.47% and 89.80%). The SP has shown a better performance during this shading case as compared to BL and TCT configurations.

During building shading case C, 30.86% of the total array has been subjected to shading as shown in FIGURE 8 (a) with theoretical power output calculated as 20.71kW.

The array configurations have generated non-convex P∼V characteristics curves with four peaks as shown in FIGURE 8 (b). In this case, the TCT configuration has generated the maximum power output of 14.14kW followed by BL (13.84kW) and SP (13,49kW). Similarly, the TCT has the lowest mismatch and power losses of 8.7kW and 6.57kW respectively with higher operational and power conversion efficiencies of 12.86% and 68.27% as compared to SP and BL. However, the TCT array encountered a higher MPPT tracking loss of 12.22kW as compared to the BL (1.16kW) and SP (0.52kW).

During building shading case D as shown in FIGURE 9 (a), 61.72% of the array has been covered with the shadow generating a theoretical power output of 12.57kW. The TCT array has the highest power generation (8.86kW), operation efficiency (8.06%), conversion efficiency (70.48%) with the lowest mismatch (14.02kW) and power (3.71kW) losses. The SP array has generated a lower power output (8.76kW) with higher mismatch (14.12kW)

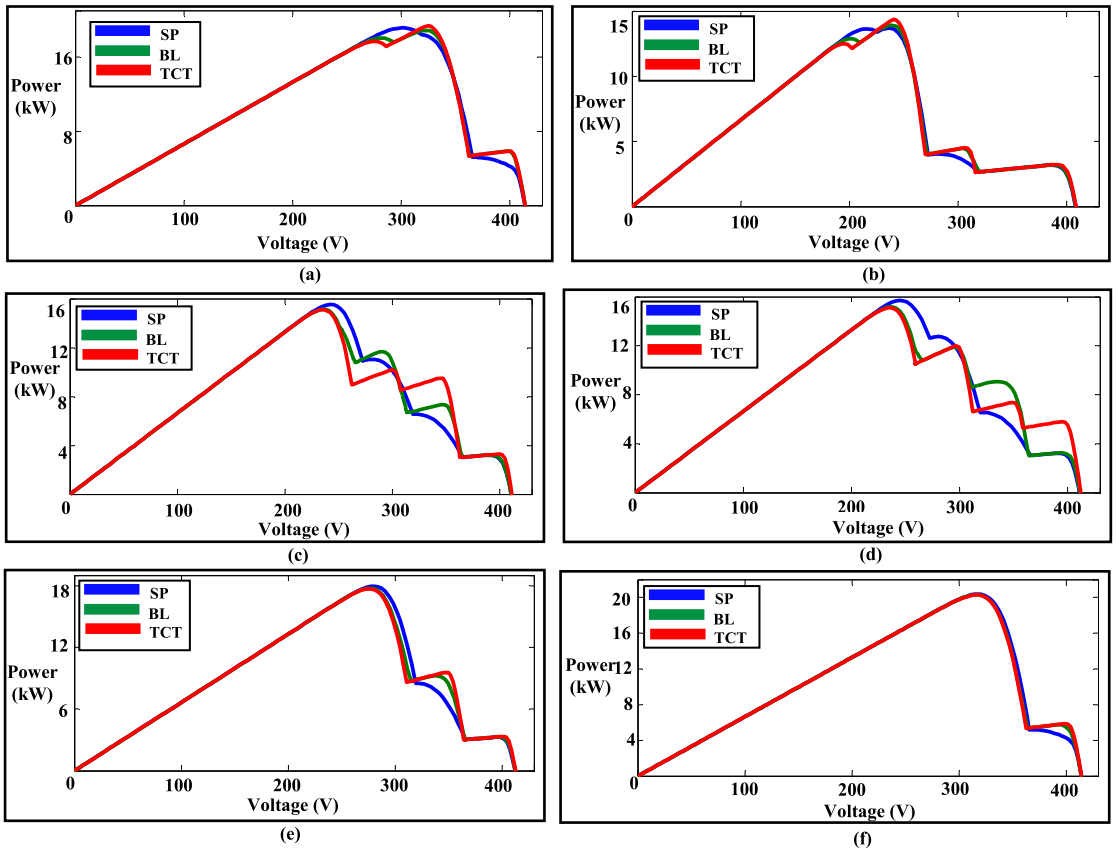


**FIGURE 11.** Power-Voltage (P∼V) characteristics curves of conventional configurations during various cloud shading scenarios. (a) Shading case A, (b) Shading case B, (c) Shading case C, (d) Shading case D, (e) Shading case E, and (f) Shading case F.

**TABLE 4.** Performance summarization of different conventional PV array configurations during cloud shading cases.

| *Cloud Shading Case A* | | | | | | | | |
|---|---|---|---|---|---|---|---|---|
| **Configuration** | **$P_T$ (kW)** | **$P_M$ (kW)** | **ML (kW)** | **PL (kW)** | **TL (kW)** | **$\eta_o$ (%)** | **$\eta_c$ (%)** | **No. of Peaks** |
| **SP** | 20.46 | 19.14 | 3.74 | 1.32 | 0 | 17.41 | 93.54 | 3 |
| **BL** | | 18.87 | 4.01 | 1.59 | 0.83 | 17.17 | 92.22 | 3 |
| **TCT** | | 19.37 | 3.51 | 1.09 | 1.68 | 17.62 | 94.67 | 3 |
| *Cloud Shading Case B* | | | | | | | | |
| **Configuration** | **$P_T$ (kW)** | **$P_M$ (kW)** | **ML (kW)** | **PL (kW)** | **TL (kW)** | **$\eta_o$ (%)** | **$\eta_c$ (%)** | **No. of Peaks** |
| **SP** | 16.51 | 13.70 | 9.18 | 2.81 | 0.07 | 12.26 | 82.98 | 4 |
| **BL** | | 13.91 | 8.97 | 2.60 | 1.02 | 12.65 | 84.25 | 4 |
| **TCT** | | 14.36 | 8.52 | 2.15 | 1.90 | 13.06 | 86.97 | 4 |
| *Cloud Shading Case C* | | | | | | | | |
| **Configuration** | **$P_T$ (kW)** | **$P_M$ (kW)** | **ML (kW)** | **PL (kW)** | **TL (kW)** | **$\eta_o$ (%)** | **$\eta_c$ (%)** | **No. of Peaks** |
| **SP** | 18.73 | 15.54 | 7.34 | 3.19 | 0 | 14.14 | 82.96 | 4 |
| **BL** | | 15.14 | 7.74 | 3.59 | 0 | 13.77 | 80.83 | 4 |
| **TCT** | | 15.10 | 7.78 | 3.63 | 0 | 13.73 | 80.61 | 4 |
| *Cloud Shading Case D* | | | | | | | | |
| **Configuration** | **$P_T$ (kW)** | **$P_M$ (kW)** | **ML (kW)** | **PL (kW)** | **TL (kW)** | **$\eta_o$ (%)** | **$\eta_c$ (%)** | **No. of Peaks** |
| **SP** | 18.24 | 15.70 | 7.18 | 2.54 | 0 | 14.28 | 86.07 | 4 |
| **BL** | | 15.18 | 7.70 | 3.06 | 0 | 13.81 | 83.22 | 4 |
| **TCT** | | 15.10 | 7.78 | 3.14 | 0 | 13.73 | 82.78 | 4 |
| *Cloud Shading Case E* | | | | | | | | |
| **Configuration** | **$P_T$ (kW)** | **$P_M$ (kW)** | **ML (kW)** | **PL (kW)** | **TL (kW)** | **$\eta_o$ (%)** | **$\eta_c$ (%)** | **No. of Peaks** |
| **SP** | 18.98 | 17.94 | 4.94 | 1.04 | 0 | 16.32 | 94.52 | 3 |
| **BL** | | 17.73 | 5.15 | 1.25 | 0 | 16.13 | 93.41 | 3 |
| **TCT** | | 17.69 | 5.19 | 1.29 | 0 | 16.09 | 93.20 | 3 |
| *Cloud Shading Case F* | | | | | | | | |
| **Configuration** | **$P_T$ (kW)** | **$P_M$ (kW)** | **ML (kW)** | **PL (kW)** | **TL (kW)** | **$\eta_o$ (%)** | **$\eta_c$ (%)** | **No. of Peaks** |
| **SP** | 20.46 | 20.37 | 2.51 | 0.09 | 0 | 18.53 | 99.56 | 2 |
| **BL** | | 20.30 | 2.58 | 0.16 | 0 | 18.47 | 99.21 | 2 |
| **TCT** | | 20.29 | 2.59 | 0.17 | 0 | 18.46 | 99.16 | 2 |

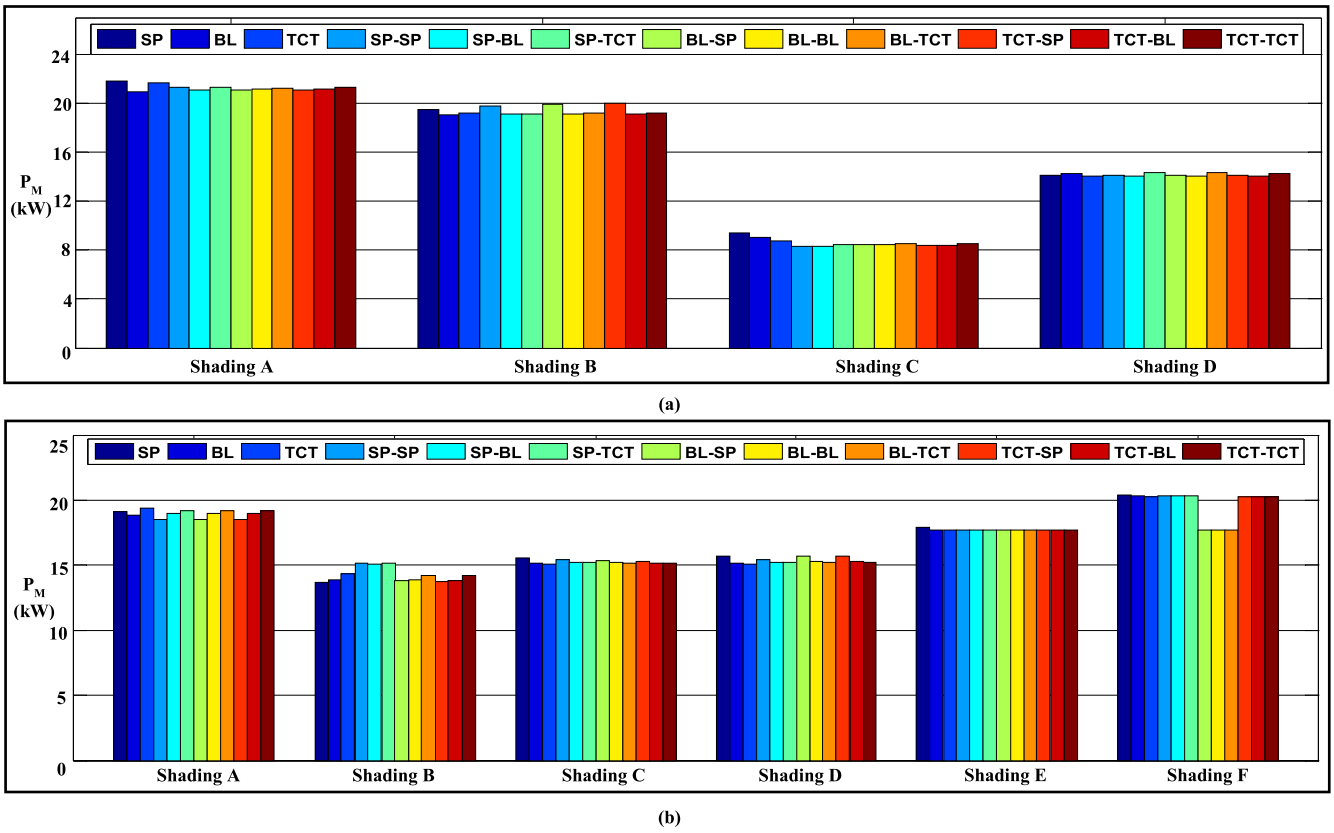


**FIGURE 12.** Comparison of maximum power generation by conventional and hybrid configurations during (a) building, and (b) cloud shading.

and power (3.81kW) losses. However, the TCT configuration has the highest tracking loss (7.31kW) as compared to SP (7.1kW) and BL (6.94kW) configurations as the P∼V characteristics curves exhibits multiple peaks as shown in FIGURE 9 (b).

The overall performance of the conventional array configurations i.e. SP, BL and TCT during building shading cases are given in Table 2. The performance evaluation of the hybrid topologies during the four building shading cases have been given in Table 3.

Among the hybrid configurations, TCT-TCT has generated the higher power whereas SP-SP, SP-BL, SP-TCT, BL-SP, BL-BL, BL-TCT, TCT-SP, and TCT-BL configurations have generated 21.28kW, 21.10kW, 21.27kW, 21.10kW, 21.14kW, 21.20kW, 21.05kW, and 21.14kW respectively. During shading B, TCT-SP has the highest power generation followed by BL-SP i.e. 19.94kW whereas SP-BL, BL-BL and TCT-BL have the lowest power generation nearly equal to 19.09kW. SP-SP configuration has the generated higher power output of 14.60kW whereas BL-BL generated a lower power output of 14.32kW during shading case C. Similarly, SP-BL, BL-BL, and TCT-BL have generated the higher power of 8.80kW followed by SP-SP, BL-SP and TCT-SP i.e. 8.76kW during shading case D.

## IV. PERFORMANCE EVALUATION UNDER CLOUDS SHADOW SCENARIO

The array configurations are tested under cloud scenarios shown in FIGURE 10 where the clouds are assumed to be flowing from the top of the array to the bottom. The modules under cloud shadow are considered to operate under 100W/m$^2$ and 40°C whereas unshaded modules are operated at 800W/m$^2$ and 45°C.

During cloud shading case A (FIGURE 10 (a)), the maximum theoretical power generation of the 9 × 9 PV array has been calculated as 20.46kW. The maximum power generation of TCT configuration is higher i.e. 19.37kW as compared to SP (19.14kW) and BL (18.87kW). The P∼V characteristics curves depicted in FIGURE 11 (a) clearly states the presence of three peaks due to which the BL and TCT configurations encountered tracking losses equal to 0.83kW and 1.68kW respectively. However, the TCT configuration encountered the lowest mismatch and power losses of 3.51kW and 1.09kW respectively as compared to SP and BL.

Similarly, the power generation of TCT configuration during cloud shading case B (as shown in FIGURE 10 (b)) is higher i.e. 14.36kW as compared to BL (13.91kW) and SP (13.70kW) configurations. However, TCT configuration encountered a higher tracking loss of 1.90kW as compared to the BL (1.02kW) and SP (0.07kW) configurations.

**TABLE 5.** Performance summarization of different hybrid PV array configurations during cloud shading cases.

| *Cloud Shading Case A* | | | | | | | | |
|---|---|---|---|---|---|---|---|---|
| **Configuration** | **$P_T$ (kW)** | **$P_M$ (kW)** | **ML (kW)** | **PL (kW)** | **TL (kW)** | **$\eta_o$ (%)** | **$\eta_c$ (%)** | **No. of Peaks** |
| **SP-SP** | | 18.54 | 4.34 | 1.92 | 1.62 | 16.86 | 90.61 | 3 |
| **SP-BL** | | 19.00 | 3.88 | 1.46 | 1.64 | 17.28 | 92.86 | 3 |
| **SP-TCT** | | 19.18 | 3.70 | 1.28 | 1.32 | 17.45 | 93.74 | 3 |
| **BL-SP** | | 18.53 | 4.35 | 1.93 | 1.54 | 16.86 | 90.56 | 3 |
| **BL-BL** | 20.46 | 19.00 | 3.88 | 1.46 | 1.64 | 17.28 | 92.86 | 3 |
| **BL-TCT** | | 19.20 | 3.68 | 1.26 | 1.44 | 17.47 | 93.84 | 3 |
| **TCT-SP** | | 18.51 | 4.37 | 1.95 | 1.74 | 16.84 | 90.46 | 3 |
| **TCT-BL** | | 19.01 | 3.87 | 1.45 | 1.62 | 17.29 | 92.91 | 3 |
| **TCT-TCT** | | 19.20 | 3.68 | 1.26 | 1.44 | 17.47 | 93.84 | 3 |
| *Cloud Shading Case B* | | | | | | | | |
| **Configuration** | **$P_T$ (kW)** | **$P_M$ (kW)** | **ML (kW)** | **PL (kW)** | **TL (kW)** | **$\eta_o$ (%)** | **$\eta_c$ (%)** | **No. of Peaks** |
| **SP-SP** | | 15.14 | 7.74 | 1.37 | 0 | 13.77 | 91.70 | 3 |
| **SP-BL** | | 15.12 | 7.76 | 1.39 | 0 | 13.75 | 91.58 | 3 |
| **SP-TCT** | | 15.13 | 7.75 | 1.38 | 0 | 13.76 | 91.64 | 3 |
| **BL-SP** | | 13.79 | 9.09 | 2.72 | 0.74 | 12.54 | 83.52 | 4 |
| **BL-BL** | 16.51 | 13.85 | 9.03 | 2.66 | 0.86 | 12.60 | 83.88 | 4 |
| **BL-TCT** | | 14.20 | 8.68 | 2.31 | 1.55 | 12.92 | 86.00 | 4 |
| **TCT-SP** | | 13.77 | 9.11 | 2.74 | 0.76 | 12.52 | 83.40 | 4 |
| **TCT-BL** | | 13.84 | 9.04 | 2.67 | 0.90 | 12.59 | 83.82 | 4 |
| **TCT-TCT** | | 14.21 | 8.67 | 2.30 | 1.60 | 12.92 | 86.06 | 4 |
| *Cloud Shading Case C* | | | | | | | | |
| **Configuration** | **$P_T$ (kW)** | **$P_M$ (kW)** | **ML (kW)** | **PL (kW)** | **TL (kW)** | **$\eta_o$ (%)** | **$\eta_c$ (%)** | **No. of Peaks** |
| **SP-SP** | | 15.42 | 7.46 | 3.31 | 0 | 14.03 | 93.39 | 4 |
| **SP-BL** | | 15.20 | 7.68 | 3.53 | 0 | 13.83 | 92.06 | 4 |
| **SP-TCT** | | 15.23 | 7.65 | 3.50 | 0 | 13.85 | 92.24 | 4 |
| **BL-SP** | | 15.34 | 7.54 | 3.39 | 0 | 13.95 | 92.91 | 4 |
| **BL-BL** | 18.73 | 15.19 | 7.69 | 3.54 | 0 | 13.82 | 92.00 | 4 |
| **BL-TCT** | | 15.18 | 7.70 | 3.55 | 0 | 13.81 | 91.94 | 4 |
| **TCT-SP** | | 15.31 | 7.57 | 3.42 | 0 | 13.93 | 92.73 | 4 |
| **TCT-BL** | | 15.15 | 7.73 | 3.58 | 0 | 13.78 | 91.76 | 4 |
| **TCT-TCT** | | 15.14 | 7.74 | 3.59 | 0 | 13.77 | 91.70 | 4 |
| *Cloud Shading Case D* | | | | | | | | |
| **Configuration** | **$P_T$ (kW)** | **$P_M$ (kW)** | **ML (kW)** | **PL (kW)** | **TL (kW)** | **$\eta_o$ (%)** | **$\eta_c$ (%)** | **No. of Peaks** |
| **SP-SP** | | 15.45 | 7.43 | 3.28 | 0 | 14.05 | 82.48 | 4 |
| **SP-BL** | | 15.22 | 7.66 | 3.51 | 0 | 13.84 | 81.26 | 4 |
| **SP-TCT** | | 15.22 | 7.66 | 3.51 | 0 | 13.84 | 81.26 | 4 |
| **BL-SP** | | 15.70 | 7.18 | 3.03 | 0 | 14.28 | 83.82 | 4 |
| **BL-BL** | | 15.28 | 7.60 | 3.45 | 0 | 13.90 | 81.58 | 4 |
| **BL-TCT** | 18.24 | 15.21 | 7.67 | 3.52 | 0 | 13.83 | 81.20 | 4 |
| **TCT-SP** | | 15.69 | 7.19 | 3.04 | 0 | 14.27 | 83.76 | 4 |
| **TCT-BL** | | 15.28 | 7.60 | 3.45 | 0 | 13.90 | 81.58 | 4 |
| **TCT-TCT** | | 15.20 | 7.68 | 3.53 | 0 | 13.83 | 81.15 | 4 |
| *Cloud Shading Case E* | | | | | | | | |
| **Configuration** | **$P_T$ (kW)** | **$P_M$ (kW)** | **ML (kW)** | **PL (kW)** | **TL (kW)** | **$\eta_o$ (%)** | **$\eta_c$ (%)** | **No. of Peaks** |
| **SP-SP** | | 17.74 | 5.14 | 1.24 | 0 | 16.14 | 93.46 | 3 |
| **SP-BL** | | 17.74 | 5.14 | 1.24 | 0 | 16.14 | 93.46 | 3 |
| **SP-TCT** | | 17.73 | 5.15 | 1.25 | 0 | 16.13 | 93.41 | 3 |
| **BL-SP** | | 17.73 | 5.15 | 1.25 | 0 | 16.13 | 93.41 | 3 |
| **BL-BL** | 18.98 | 17.72 | 5.16 | 1.26 | 0 | 16.12 | 93.36 | 3 |
| **BL-TCT** | | 17.72 | 5.16 | 1.26 | 0 | 16.12 | 93.36 | 3 |
| **TCT-SP** | | 17.70 | 5.18 | 1.28 | 0 | 16.10 | 93.25 | 3 |
| **TCT-BL** | | 17.69 | 5.19 | 1.29 | 0 | 16.09 | 93.20 | 3 |
| **TCT-TCT** | | 17.69 | 5.19 | 1.29 | 0 | 16.09 | 93.20 | 3 |
| *Cloud Shading Case F* | | | | | | | | |
| **Configuration** | **$P_T$ (kW)** | **$P_M$ (kW)** | **ML (kW)** | **PL (kW)** | **TL (kW)** | **$\eta_o$ (%)** | **$\eta_c$ (%)** | **No. of Peaks** |
| **SP-SP** | | 20.31 | 2.57 | 0.15 | 0 | 18.48 | 99.26 | 2 |
| **SP-BL** | | 20.31 | 2.57 | 0.15 | 0 | 18.48 | 99.26 | 2 |
| **SP-TCT** | | 20.31 | 2.57 | 0.15 | 0 | 18.48 | 99.26 | 2 |
| **BL-SP** | | 17.73 | 5.15 | 2.73 | 0 | 16.13 | 86.65 | 3 |
| **BL-BL** | 20.46 | 17.72 | 5.16 | 2.74 | 0 | 16.12 | 86.60 | 3 |
| **BL-TCT** | | 17.72 | 5.16 | 2.74 | 0 | 16.12 | 86.60 | 3 |
| **TCT-SP** | | 20.29 | 2.59 | 0.17 | 0 | 18.46 | 99.16 | 2 |
| **TCT-BL** | | 20.29 | 2.59 | 0.17 | 0 | 18.46 | 99.16 | 2 |
| **TCT-TCT** | | 20.29 | 2.59 | 0.17 | 0 | 18.46 | 99.16 | 2 |

The P∼V curves of the configurations exhibited four peaks as shown in FIGURE 11 (b) with SP experiencing the higher mismatch (3.74kW) and power (1.32kW) losses.

The cloud shading case C has been represented in FIGURE 10 (c) and the P∼V curves of the configurations during that particular scenario are represented in FIGURE 11 (c). The power generation of the SP array is found to be maximum i.e. 15.54kW with lower mismatch (7.34kW) and power (3.19kW) losses as compared to the BL and TCT. Similarly, the array with SP configuration has higher operational and conversion efficiencies of 14.14% and 82.96%. Also, all the array configurations have encountered zero tracking losses as the actual MPP is located at the first position in the curves.

Similarly, the cloud shading cases D, E, and F for the 9 × 9 PV array configurations have been shown in FIGURE 10 (d), (e), and (f) respectively. The P∼V characteristics curves of the shading D, E, and F are depicted in FIGURE 11 (d), (e), and (f) respectively. The SP configuration has the highest power generation during shading D, E, and F i.e. 15.70kW, 17.94kW, and 20.37kW respectively as compared to BL and TCT. Also, the SP has the lower mismatch and power losses with higher operational and power conversion efficiencies during shading cases D, E and F as compared to BL and TCT configurations. The configurations encountered zero tracking losses during the three cloud shading cases as the actual MPP of the system lies in the first peak of the characteristics curves.

The performances of the conventional interconnection configurations during all the cloud shading cases have been summarized in TABLE 4.

TABLE 5 represents the summarized performances of all the hybrid interconnection configurations during different cloud shading cases. During shading A and B, the BL-TCT and TCT-TCT have equally generated higher power of 19.20kW and 14.21kW respectively. The SP-SP array has generated higher power during shading C whereas BL-SP has the higher performance during shading D. During shading F, SP-SP and SP-BL have the higher power generation of 17.74kW whereas the SP-SP, SP-BL and SP-TCT have generated maximum power (20.31kW) during shading G.

## V. PERFORMANCE COMPARISON OF PV ARRAY CONFIGURATIONS

The performance comparison of conventional and hybrid configurations are done in term of power generation, tracking losses and redundancy level. The comparison has been done to determine the most optimal configuration for a roof-top PV array system during partial shading scenarios caused by the neighbouring buildings and clouds.

FIGURE 12 (a) and (b) represents the maximum power generation comparisons of the 9 × 9 arrays during building and cloud coverage shading scenarios. From the graphs, it can be established that in most of the shading cases, SP has the higher maximum power generation. During building shading cases, SP has the higher power generation during all the cases whereas, in the case of the cloud coverage, the power generation of SP is found to be maximum during all shading cases except shading B.

**TABLE 6. Extra wires, Knots and losses probability of array configurations.**

| Configurations | Extra Wires | Extra Knots | Redundancy level and Wiring Losses |
|---|---|---|---|
| SP | 0 | 0 | Low |
| BL | 32 | 64 | High |
| TCT | 64 | 72 | High |
| SP-SP | 0 | 0 | Low |
| SP-BL | 2 | 4 | Low |
| SP-TCT | 4 | 6 | Low |
| BL-SP | 18 | 36 | Medium |
| BL-BL | 20 | 40 | Medium |
| BL-TCT | 22 | 42 | Medium |
| TCT-SP | 36 | 54 | High |
| TCT-BL | 38 | 58 | High |
| TCT-TCT | 40 | 60 | High |

FIGURE 13 (a) and (b) indicates the comparative graphs of tracking losses encountered by the array configurations during neighbouring building and cloud scenarios. During building shading cases, SP has encountered the lowest MPPT tracking power losses except for shading D which is nearly equal to all other scenarios. However, during cloud scenarios, SP has generated zero tracking losses during all the cases.'

The SP array configuration has encountered the lowest mismatch and power losses in most of the shading cases. It is found that the SP configuration has encountered the lowest mismatch and power losses during building shading cases A and B as compared to all other configurations whereas there is a slightly higher mismatch and power loss as compared to TCT during cases C and D. Similarly, SP have the lowest mismatch and power losses during all the shading cases caused by the clouds except case A and B where TCT has slightly lower losses.

The redundancy levels of all the configurations in terms of extra wires, extra knots and wiring losses probability have been given in TABLE 6. SP and SP-SP configurations require no extra wires and hence, the redundancy level and wiring losses are low. In the case of the SP-BL and SP-TCT, the extra wires required in the configurations have been found as 0, 2 and 4 respectively and hence, encounter low wiring losses and redundancy. The BL, TCT, TCT-SP, TCT-BL and TCT-TCT configurations have higher wiring losses and redundancy levels due to the presence of a higher number of wires in the system.

Hence, from the above study and results obtained, it can be concluded that the SP configuration has the maximum power generation with low system losses and redundancy levels. TCT architectures have encountered higher losses probability and redundancy and hence can add complexity to the system. The BL configuration has shown medium performance and cannot be considered as reliable topology during partial shading scenarios in the roof-top PV system. Hence, for better

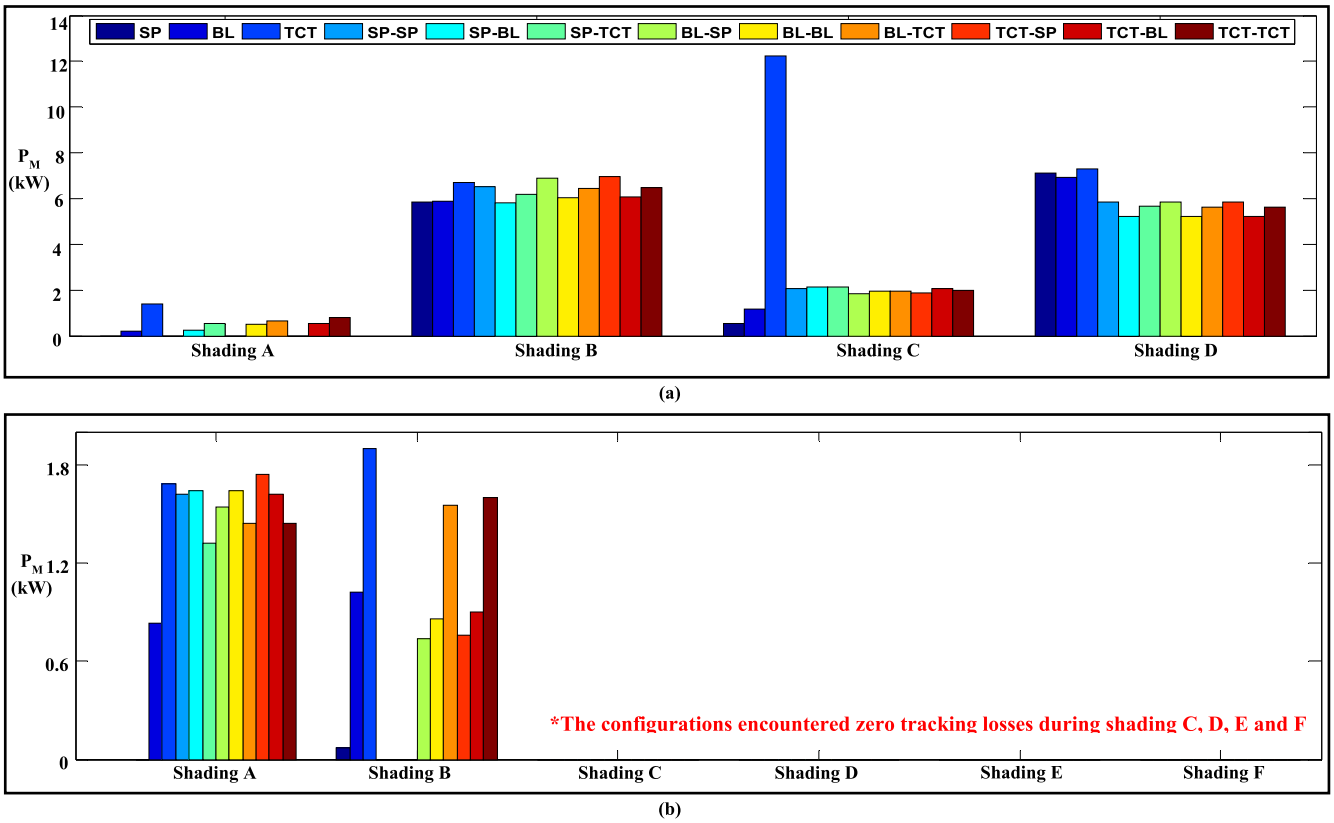


**FIGURE 13.** Comparison of MPPT tracking losses encountered by conventional and hybrid configurations during (a) building, and (b) cloud shading.

performance, reliability and reduced complexity, the SP can be the most optimal configuration for implementing in the roof-top PV arrays.

## VI. CONCLUSION

In this study, the widely accepted conventional and hybrid array interconnection configurations are studied for a 9 × 9 roof-top based array. The configurations mainly include SP, BL, TCT, SP-SP, SP-BL, SP-TCT, BL-SP, BL-BL, BL-TCT, TCT-SP, TCT-BL and TCT-TCT configurations. The investigation is conducted for uneven shading scenarios caused by neighbouring buildings and cloud shadows for a 9 × 9 array in the MATLAB/Simulink environment. The major findings of the conducted analysis are as follows:

- Series-Parallel (SP) has generated notable higher power during most of the building based shading scenarios covering 1.23%, and 7.40% whereas total cross tied (TCT) has generated only a slightly higher power (in some W from kW system) during 30.86% and 61.72% shadings.
- During the cloud shading scenario, SP generated the maximum power during most of the shading cases with shading strength of 11.11%, 18.51%, 24.69%, and 22.22% whereas TCT generated a slightly higher power than SP during 30.86% shading.
- SP configuration has the higher power conversion and operational efficiencies during most of the shading compared to any conventional and hybrid configurations.
- SP configuration has a very low redundancy due to the presence of no extra wires and knots indicating zero wiring losses possibility. However, TCT and other topologies have higher possibilities of wiring losses due to the presence of wires and knots. Also, these configurations have higher redundancy that can lead to complexity and difficulties in fault diagnosis.
- In the existing literature, TCT configuration has been proved to yield higher power during shading as compared to any other configuration. However, the higher power generation of TCT is limited to even shading patterns and remains inapplicable in case of uneven shadings caused by buildings and clouds shadows.
- The performance of the configurations depends on the pattern, strength and area of the shading.

Hence, from the investigation, it can be concluded that the interconnection configurations has a puny effect on the power generation of the roof-top PV array during uneven shading scenarios caused by neighbouring buildings. So, SP is found to be the most optimal configuration for roof-top based arrays due to its higher power generation capability during uneven shading cases, low losses, low redundancy, low complexity and easy fault detection characteristics.

## REFERENCES

[1] A. Kumar Behura, A. Kumar, D. Kumar Rajak, C. I. Pruncu, and L. Lamberti, "Towards better performances for a novel rooftop solar PV system," *Sol. Energy*, vol. 216, pp. 518–529, Mar. 2021.

[2] R. J. Mustafa, M. R. Gomaa, M. Al-Dhaifallah, and H. Rezk, "Environmental impacts on the performance of solar photovoltaic systems," *Sustainability*, vol. 12, no. 2, p. 608, Jan. 2020.
[3] K. A. K. Niazi, W. Akhtar, H. A. Khan, Y. Yang, and S. Athar, "Hotspot diagnosis for solar photovoltaic modules using a naive Bayes classifier," *Sol. Energy*, vol. 190, pp. 34–43, Sep. 2019.
[4] P. R. Satpathy, R. Sharma, S. K. Panigrahi, and S. Panda, "Bypass diodes configurations for mismatch and hotspot reduction in PV modules," in *Proc. Int. Conf. Comput. Intell. Smart Power Syst. Sustain. Energy (CISPSSE)*, Jul. 2020, pp. 1–6.
[5] A. Mohapatra, B. Nayak, P. Das, and K. B. Mohanty, "A review on MPPT techniques of PV system under partial shading condition," *Renew. Sustain. Energy Rev.*, vol. 80, pp. 854–867, Dec. 2017.
[6] Y.-P. Huang, M.-Y. Huang, and C.-E. Ye, "A fusion firefly algorithm with simplified propagation for photovoltaic MPPT under partial shading conditions," *IEEE Trans. Sustain. Energy*, vol. 11, no. 4, pp. 2641–2652, Oct. 2020.
[7] M. Mansoor, A. F. Mirza, and Q. Ling, "Harris hawk optimization-based MPPT control for PV systems under partial shading conditions," *J. Cleaner Prod.*, vol. 274, Nov. 2020, Art. no. 122857.
[8] M. Mansoor, A. F. Mirza, Q. Ling, and M. Y. Javed, "Novel grass hopper optimization based MPPT of PV systems for complex partial shading conditions," *Sol. Energy*, vol. 198, pp. 499–518, Mar. 2020.
[9] A. F. Mirza, M. Mansoor, Q. Ling, B. Yin, and M. Y. Javed, "A salp-swarm optimization based MPPT technique for harvesting maximum energy from PV systems under partial shading conditions," *Energy Convers. Manage.*, vol. 209, Apr. 2020, Art. no. 112625.
[10] Z. Zhao, R. Cheng, B. Yan, J. Zhang, Z. Zhang, M. Zhang, and L. L. Lai, "A dynamic particles MPPT method for photovoltaic systems under partial shading conditions," *Energy Convers. Manage.*, vol. 220, Sep. 2020, Art. no. 113070.
[11] M. Joisher, D. Singh, S. Taheri, D. R. Espinoza-Trejo, E. Pouresmaeil, and H. Taheri, "A hybrid evolutionary-based MPPT for photovoltaic systems under partial shading conditions," *IEEE Access*, vol. 8, pp. 38481–38492, 2020.
[12] K. Guo, L. Cui, M. Mao, L. Zhou, and Q. Zhang, "An improved gray wolf optimizer MPPT algorithm for PV system with BFBIC converter under partial shading," *IEEE Access*, vol. 8, pp. 103476–103490, 2020.
[13] A. M. Eltamaly, M. S. Al-Saud, and A. G. Abokhalil, "A novel bat algorithm strategy for maximum power point tracker of photovoltaic energy systems under dynamic partial shading," *IEEE Access*, vol. 8, pp. 10048–10060, 2020.
[14] D. Yousri, T. S. Babu, D. Allam, V. K. Ramachandaramurthy, and M. B. Etiba, "A novel chaotic flower pollination algorithm for global maximum power point tracking for photovoltaic system under partial shading conditions," *IEEE Access*, vol. 7, pp. 121432–121445, 2019.
[15] D. Yousri, T. S. Babu, E. Beshr, M. B. Eteiba, and D. Allam, "A robust strategy based on marine predators algorithm for large scale photovoltaic array reconfiguration to mitigate the partial shading effect on the performance of PV system," *IEEE Access*, vol. 8, pp. 112407–112426, 2020.
[16] G. Sai Krishna and T. Moger, "Reconfiguration strategies for reducing partial shading effects in photovoltaic arrays: State of the art," *Sol. Energy*, vol. 182, pp. 429–452, Apr. 2019.
[17] H. Ali and H. A. Khan, "Analysis on inverter selection for domestic rooftop solar photovoltaic system deployment," *Int. Trans. Elect. Energy Syst.*, vol. 30, May 2020, Art. no. e12351.
[18] A. Mansur, M. Amin, and K. Islam, "Performance comparison of mismatch power loss minimization techniques in series-parallel PV array configurations," *Energies*, vol. 12, no. 5, p. 874, Mar. 2019.
[19] P. R. Satpathy, S. Jena, and R. Sharma, "Power enhancement from partially shaded modules of solar PV arrays through various interconnections among modules," *Energy*, vol. 144, pp. 839–850, Feb. 2018.
[20] F. Belhachat and C. Larbes, "Modeling, analysis and comparison of solar photovoltaic array configurations under partial shading conditions," *Sol. Energy*, vol. 120, pp. 399–418, Oct. 2015.
[21] M. Dhimish, V. Holmes, B. Mehrdadi, M. Dales, B. Chong, and L. Zhang, "Seven indicators variations for multiple PV array configurations under partial shading and faulty PV conditions," *Renew. Energy*, vol. 113, pp. 438–460, Dec. 2017.
[22] K. Lappalainen and S. Valkealahti, "Photovoltaic mismatch losses caused by moving clouds," *Sol. Energy*, vol. 158, pp. 455–461, Dec. 2017.
[23] R. K. Pachauri, O. P. Mahela, A. Sharma, J. Bai, Y. K. Chauhan, B. Khan, and H. H. Alhelou, "Impact of partial shading on various PV array configurations and different modeling approaches: A comprehensive review," *IEEE Access*, vol. 8, pp. 181375–181403, 2020.
[24] P. R. Satpathy, R. Sharma, and S. Jena, "A shade dispersion interconnection scheme for partially shaded modules in a solar PV array network," *Energy*, vol. 139, pp. 350–365, Nov. 2017.
[25] A. S. Yadav, R. K. Pachauri, Y. K. Chauhan, S. Choudhury, and R. Singh, "Performance enhancement of partially shaded PV array using novel shade dispersion effect on magic-square puzzle configuration," *Sol. Energy*, vol. 144, pp. 780–797, Mar. 2017.
[26] P. R. Satpathy and R. Sharma, "Power loss reduction in partially shaded PV arrays by a static SDP technique," *Energy*, vol. 156, pp. 569–585, Aug. 2018.
[27] P. Satpathy, R. Sharma, and S. Dash, "An efficient sd-par technique for maximum power generation from modules of partially shaded pv arrays," *Energy*, vol. 175, pp. 182–194, 2019.
[28] S. G. Krishna and T. Moger, "Optimal SuDoKu reconfiguration technique for total-cross-tied PV array to increase power output under non-uniform irradiance," *IEEE Trans. Energy Convers.*, vol. 34, no. 4, pp. 1973–1984, Dec. 2019.
[29] P. R. Satpathy and R. Sharma, "Power and mismatch losses mitigation by a fixed electrical reconfiguration technique for partially shaded photovoltaic arrays," *Energy Convers. Manage.*, vol. 192, pp. 52–70, Jul. 2019.
[30] R. Venkateswari and N. Rajasekar, "Power enhancement of PV system via physical array reconfiguration based Lo Shu technique," *Energy Convers. Manage.*, vol. 215, Jul. 2020, Art. no. 112885.
[31] S. Ghosh, V. K. Yadav, and V. Mukherjee, "Evaluation of cumulative impact of partial shading and aerosols on different PV array topologies through combined Shannon's entropy and DEA," *Energy*, vol. 144, pp. 765–775, Feb. 2018.
[32] M. Premkumar, U. Subramaniam, T. S. Babu, R. M. Elavarasan, and L. Mihet-Popa, "Evaluation of mathematical model to characterize the performance of conventional and hybrid PV array topologies under static and dynamic shading patterns," *Energies*, vol. 13, no. 12, p. 3216, Jun. 2020.
[33] P. R. Satpathy, T. S. Babu, A. Mahmoud, R. Sharma, and B. Nastasi, "A TCT-SC hybridized voltage equalizer for partial shading mitigation in PV arrays," *IEEE Trans. Sustain. Energy*, vol. 12, no. 4, pp. 2268–2281, Oct. 2021.

**PRIYA RANJAN SATPATHY** received the B.Tech. degree in electrical engineering and M.Tech. degree in renewable engineering and management, in 2015 and 2017, respectively. He is currently pursuing the Ph.D. degree in solar photovoltaic system (electrical engineering) with Siksha 'O' Anusandhan (Deemed to be University), India. He is currently a Senior Research Fellow (SRF) with the Council of Scientific and Industrial Research (CSIR), Government of India. He has depth knowledge on different PV system software, such as PVSyst, PVSOL, Sketchup, HelioScope, and AutoCAD. He has been reviewed more than 100 articles of various reputed conferences and journals, such as IEEE, IET, Elsevier, Wiley, Springer, Taylor and Francis, and Hindawi in a span of three years. His research interests include solar PV power system, PV array efficiency improvement and fault reduction, maximum power point tracking, and PV system (off-grid and on-grid) design and installation.

**THANIKANTI SUDHAKAR BABU** (Senior Member, IEEE) received the B.Tech. degree from Jawaharlal Nehru Technological University Anantapur, India, in 2009, the M.Tech. degree in power electronics and industrial drives from Anna University, Chennai, India, in 2011, and the Ph.D. degree from VIT University, Vellore, India, in 2017.

He is currently working as an Associate Professor with the Department of Electrical Engineering, Chaitanya Bharathi Institute of Technology (CBIT), Hyderabad, India. He had completed his Postdoctoral Research Fellowship from the Institute of Power Engineering, Universiti Tenaga Nasional (UNITEN), Malaysia. Prior to that, he worked as an Assistant Professor at the School of Electrical Engineering, VIT University. He has published more than 80 research articles in various renowned international journals. His research interests include design and implementation of solar PV systems, renewable energy resources, power management for hybrid energy systems, storage systems, fuel cell technologies, electric vehicles, and smart grids. He has been acting as an Associate Editor of *IET Renewable Power Generation* (RPG), IEEE Access, *International Transactions on Electrical Energy Systems* (Willey), and *Frontiers in Energy Research*, a Section Editor of *Energies* (MDPI) and *Sustainability* (MDPI), and a reviewer of various reputed journals.

**SATHISH KUMAR SHANMUGAM** received the Ph.D. degree from the Faculty of Information and Communication Engineering, Anna University, Chennai, India, in 2017. He is currently working as an Associate Professor with the Department of EEE, M. Kumarasamy College of Engineering, Karur, Tamil Nadu, India. He published 15 SCIE, 20 Scopus papers in reputed journals. He has 16 years of teaching experience. His current research interests include control, embedded systems, modeling, and power electronics converter. In addition, he is a Reviewer of IEEE Transactions of Industrial Electronics, IEEE Access, *ETRI Journal*, *Journal of Electrical Engineering & Technology*, *JVE*, *JME*, *MME*, and *ITEES*.

**LAKSHMAN NAIK POPAVATH** received the bachelor's degree in electrical and electronics engineering from GITAM College of Engineering, India, in 2008, the Post Graduate Diploma degree in energy management (PGDENM) from the Central University of Hyderabad, India, in 2010, the master's degree (Hons.) in electrical engineering from JNTU Kakinada, India, in 2012, and the Ph.D. degree in electrical engineering from VIT University Vellore, India. He is currently working as an Associate Professor with the Department of Electrical and Electronics Engineering, Vasireddy Venkatadri Institute of Technology (VVIT), Nambur, India. He has authored 20 scientific papers in refereed international journals and conference proceedings in the field of green energy, power quality improvement, electric vehicles, and power electronics.

**HASSAN HAES ALHELOU** (Senior Member, IEEE) is currently with the School of Electrical and Electronic Engineering, University College Dublin, Ireland. He is a Faculty Member at Tishreen University, Lattakia, Syria. He has participated in more than 15 industrial projects. He has published more than 150 research articles in high-quality peer-reviewed journals and international conferences. He is included in the 2018 Publons list of the top 1% best reviewer and researchers in the field of engineering in the world. He has also performed more than 600 reviews for high prestigious journals, including IEEE Transactions on Industrial Informatics, IEEE Transactions on Industrial Power Systems, and *International Journal of Electrical Power & Energy Systems*. His research interests include power system operation, power system dynamics and control, smart grids, microgrids, demand response, and load shedding. He was a recipient of the Outstanding Reviewer Award from many journals, such as *Energy Conversion and Management* (ECM) and *ISA Transactions, and Applied Energy*. He was also a recipient of the Best Young Researcher in the Arab Student Forum Creative among 61 researchers from 16 countries at Alexandria University, Egypt, in 2011.